

# Comparative population genetics of congeneric limpets across a biogeographic transition zone reveals common patterns of genetic structure and demographic history

Livia Peluso<sup>1,2</sup> | Bernardo R. Broitman<sup>3,4,5</sup> | Marco A. Lardies<sup>3,4</sup> | Roberto F. Nespolo<sup>1,6</sup> | Pablo Saenz-Agudelo<sup>1,7</sup>

<sup>1</sup>Instituto de Ciencias Ambientales y Evolutivas, Universidad Austral de Chile, Valdivia, Chile

<sup>2</sup>Escuela de Graduados, Facultad de Ciencias, Universidad Austral de Chile, Valdivia, Chile

<sup>3</sup>Departamento de Ciencias, Facultad de Artes Liberales, Universidad Adolfo Ibáñez, Santiago, Chile

<sup>4</sup>Millennium Institute SECOS, Santiago, Chile

<sup>5</sup>Millennium Nucleus UPWELL, Santiago, Chile

<sup>6</sup>Millennium Nucleus LiLi, Valdivia, Chile

<sup>7</sup>Millennium Nucleus NUTME, Santiago, Chile

## Correspondence

Pablo Saenz-Agudelo, Instituto de Ciencias Ambientales y Evolutivas, Universidad Austral de Chile, Valdivia, Chile.  
Email: [pablo.saenzagudelo@gmail.com](mailto:pablo.saenzagudelo@gmail.com)

## Funding information

Comisión Nacional de Investigación Científica y Tecnológica, Grant/Award Number: 21170187; Fondo Nacional de Desarrollo Científico y Tecnológico, Grant/Award Number: 1190710

Handling Editor: Cynthia Riginos

## Abstract

The distribution of genetic diversity is often heterogeneous in space, and it usually correlates with environmental transitions or historical processes that affect demography. The coast of Chile encompasses two biogeographic provinces and spans a broad environmental gradient together with oceanographic processes linked to coastal topography that can affect species' genetic diversity. Here, we evaluated the genetic connectivity and historical demography of four *Scurria* limpets, *S. scurra*, *S. variabilis*, *S. cecilians* and *S. araucana*, between ca. 19°S and 53°S in the Chilean coast using genome-wide SNPs markers. Genetic structure varied among species which was evidenced by species-specific breaks together with two shared breaks. One of the shared breaks was located at 22–25°S and was observed in *S. araucana* and *S. variabilis*, while the second break around 31–34°S was shared by three *Scurria* species. Interestingly, the identified genetic breaks are also shared with other low-disperser invertebrates. Demographic histories show bottlenecks in *S. scurra* and *S. araucana* populations and recent population expansion in all species. The shared genetic breaks can be linked to oceanographic features acting as soft barriers to dispersal and also to historical climate, evidencing the utility of comparing multiple and sympatric species to understand the influence of a particular seascape on genetic diversity.

## KEYWORDS

Chile, intertidal, RADseq, rocky shores, *Scurria*, Southeastern Pacific

## 1 | INTRODUCTION

Species' genetic diversity is often heterogeneously distributed in space, a consequence of the ecological and evolutionary processes interacting in the landscape (Manel et al., 2020; Selkoe et al., 2016). For marine species that mainly depend on planktonic larvae for dispersal, it is expected that the environment is determinant of the spatial distribution of this genetic diversity, especially considering the highly variable temporal and spatial scales oceanographic features act on (Riginos & Liggins, 2013). To understand how these

oceanographic and other factors shape marine biodiversity, comparative phylogeographic and population genetic approaches provide a solid framework to study if patterns of genetic diversity and genetic divergence among populations are shared among different species with similar distributions (McGaughan et al., 2022). The spatial covariation between biogeographic partitioning and species population genetic patterns in comparative studies can help build robust tests to infer the evolutionary processes shaping species composition and population-level genetic divergence (Bowen et al., 2016; McGaughan et al., 2022).

Regions with abrupt or gradient-like changes in environmental conditions represent good natural laboratories to test if similar patterns in species' genetic structure exist and infer which processes, such as environmental restrictions, can explain these pattern similarities (Dawson et al., 2014; Haye et al., 2014). The central-northern coast of Chile in the Southeastern Pacific is one example of this, extending almost linearly for more than 2000 km from 18° to 42° S, where the smooth thermal gradient that follows the latitudinal change is a clear environmental filter (Broitman et al., 2021; Lara et al., 2019). In contrast, the coastline of southern Chile between 42° and 55° S is highly heterogeneous due to the effects of quaternary glaciations on the landscape. There is an extensive system of fjords and channels that exhibit horizontal and vertical salinity gradients due to high rainfall and sustained meltwater inflows from glaciers and icefields (Pantoja et al., 2011; Saldías et al., 2019). While the open coast of the southern fjordland is under a downwelling regime, the more homogeneous central-northern sector experiences a wind-driven upwelling regime that is semi-permanent north of 30° S and markedly seasonal between 30° and 42° S (Thiel et al., 2007). Considering these geological, environmental and community composition characteristics two biogeographic provinces are defined on the Chilean coast, the Peruvian Province (PP) and the Magellanic Province (MP) (Brattström & Johanssen, 1983; Camus, 2001). These are separated by an Intermediate Area (IA) that sets two biogeographic limits in this region, one at the end of the PP and the beginning of the IA around 30° S, and the other at the end of IA and beginning of the MP around 42° S (Camus, 2001).

Biogeographic breaks are often associated with concordant genetic structure among species that cross these boundaries (Bowen et al., 2016). Indeed such patterns have been observed in some marine invertebrates in Chile, such as *Tegula atra*, *Scurria zebrina*, *Notochthamalus scabrosus* and *Acanthina monodon* (Haye et al., 2014; Saenz-Agudelo et al., 2022; Sánchez et al., 2011; Zakas et al., 2009). Still, this pattern is not prevalent considering other invertebrates, such as *Concholepas concholepas* and *Heliaster helianthus* (Cárdenas et al., 2009; Haye et al., 2014), have no genetic structure across these limits. A recent biogeographic study in the IA region showed that the difference in inferred breaks could be due to differences in larval development, considering they found a break around 30° S associated with species with lecithotrophic larvae and another break at 34° S associated with species with planktotrophic larvae (Lara et al., 2019). Yet, phylogeographic or population genetic comparative studies in Chile are scarce and have focused on distant related taxa or species with allopatric and parapatric ranges, hindering the understanding of how common evolutionary processes shape similar genetic structure in the same space. To better understand how present and past Chilean seascapes affected the genetic diversity patterns observed today and what processes are common to sympatric species, we used patellogastropods from the genus *Scurria* Gray, 1847 as models, specifically *Scurria scurra* (Lesson, 1830), *S. variabilis* (Sowerby, 1839), *S. cecilians* (Orbigny, 1841) and *S. araucana* (Orbigny, 1841).

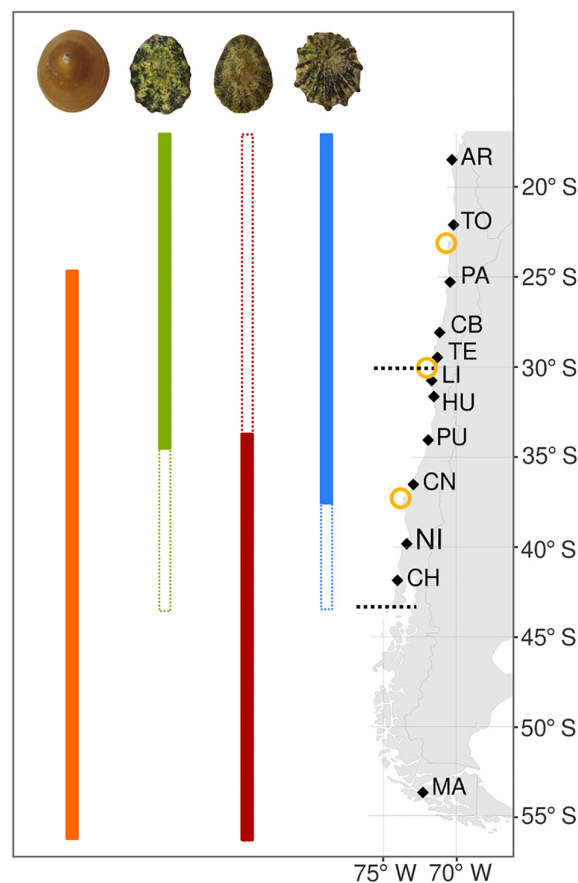


**FIGURE 1** Map illustrating the geographic range in Chile of the four *Scurria* species in this study as vertical bars, the main biogeographic breaks (dashed black horizontal lines) and the location of the major upwelling centres (yellow circles) in the studied region. Vertical colour bars indicate the geographic range described in the literature for each species (orange corresponds to *S. scurra*, green to *S. variabilis*, red to *S. cecilians* and blue to *S. araucana*). The filled section of each coloured bar indicates the geographic range covered in this study and the empty sections correspond to the reported distribution for each species where specimens were not found. AR, Arica; CB, Carrizal Bajo; CH, Chiloé; CN, Concepción; HU, Huentelauquén; LI, Limarí; MA, Magallanes; NI, Niebla; PA, Paposo; PU, Puertecillo; TE, Temblador; TO, Tocopilla.

*Scurria* limpets are common organisms in the intertidal zone of rocky shores and are endemic to the Southeast Pacific (i.e. Chile and Peru) occupying rocky substrates, or in the case of *S. scurra*, homing in the stipes of the kelps *Durvillaea* spp. and *Lessonia* spp. (Espoz et al., 2004; Valdovinos, 1999). The known geographic range of these species varies: *S. scurra* spans from 24° to 55° S, *S. variabilis* from 10° to 42° S, *S. cecilians* from 5° to 54° S and *S. araucana* from 15° to 42° S (Espoz et al., 2004; Valdovinos, 1999; Figure 1). They occur in sympatry over most of their geographic ranges and also cross the two biogeographic limits in this region, with *S. scurra*, *S. variabilis* and *S. araucana* crossing the 30° S break and *S. cecilians* and *S. scurra* crossing the 42° S break. According to a recent phylogeny, *S. scurra*, *S. cecilians* and *S. araucana* comprise a monophyletic group with a relatively recent divergence (Asorey, 2017; L. Peluso, A. Vargas, C. Asorey,

S. Rosenfeld, P. Saenz-Agudelo, unpublished data). Information on the reproductive strategies and the larval characteristics of our study species is scarce. The only information available indicates that our focal *Scurria* species are broadcast spawners (Río Cardoza, 1992) and, as most patellogastropods, they likely share a lecithotrophic larva with a pelagic duration of a few days (e.g. Kay & Emler, 2002; Kolbin & Kulikova, 2011; Kuo & Sanford, 2013; Page, 2002). Overall, comparing the distribution of genetic diversity among these four congeneric endemic species provides a unique opportunity to understand if biogeographic limits are associated with spatial genetic structure and what processes may have caused it.

Previous studies suggest that genetic diversity for *Scurria* species is spatially structured and likely linked to variation in environmental conditions. Using a partial fragment of COI, Haye et al. (2014) described a genetic barrier for *S. scurra* around 30°S. Using genome-wide SNPs to describe the genetic diversity of two species, a more recent study inferred a genetic break between 22 and 25°S for *S. viridula* and a genetic break around 33–35°S associated with signatures of divergent selection for *S. zebrina* (Saenz-Agudelo et al., 2022). The genetic breaks observed for *S. scurra* and *S. zebrina* were located within the IA, the region under the influence of seasonal upwelling, which is also characterized by important mesoscale variability and a latitudinal increase in freshwater input (Hormazabal et al., 2004; Lara et al., 2019; Saldías et al., 2016). To date, it remains unclear whether neutral (oceanographic or historic events) or adaptive (adaptation to different environmental conditions) processes are responsible for current species distributions and patterns of genetic structure. Here, using SNPs from restriction-site associated DNA sequencing (RAD-seq), we evaluated the spatial patterns of genetic diversity in four sympatric and closely related *Scurria* species. Since the focal species have similar habitats (except for *S. scurra*), similar life-history traits, and are exposed to similar environmental gradients and oceanographic settings, we hypothesized that: (1) if major historical processes had a role in shaping genetic structure, concordant timings of population splits and size changes shall be shared among spatially co-occurring species; (2) if oceanographic and environmental conditions are important drivers of current population structure, we would expect that genetic discontinuities coincide geographically among species, together with similar footprints of divergent selection (outliers) among species. Taken together, we hope this comparative framework will help find generalities in the spatial distribution of genetic diversity and demographic histories and how shared environmental and historical processes have impacted the distribution of genetic diversity in space.

## 2 | MATERIALS AND METHODS

### 2.1 | Field sampling

Individuals of *Scurria scurra*, *S. variabilis*, *S. ceciliana* and *S. araucana* were sampled throughout continental Chile, from 18.5°S to 53.6°S, thus including most of the geographic range of each species. We

selected rocky shore sites in Arica (AR), Tocopilla (TO), Paposo (PA), Carrizal Bajo (CB), Temblador (TE), Limarí (LI), Huentelauquén (HU), Puertecillo (PU), Concepción (CN), Niebla (NI), Chiloé (CH) and Magallanes (MA) (Table 1, Figure 1). Samples were collected under permit R. Ex N 2036, 2019 from the Subsecretaría de Pesca y Acuicultura (SUBPESCA) of the Chilean government. Sampling was carried out in the mid and low intertidal zone during low tide and individuals were taken directly from the rock substrate or from the stipes of the macroalgae *Durvillaea* spp. and *Lessonia* spp. in the case of *S. scurra*. Samples were placed in 100% ethanol after anaesthesia in seawater with ethanol at 5% for 10 min (Gilbertson & Wyatt, 2016).

### 2.2 | DNA extraction and sequencing

In the laboratory, the foot tissue of each individual was separated and used for DNA extraction with the GeneJET genomic DNA purification kit (ThermoFisher). DNA quality was verified with a 1% agarose gel and DNA concentration was estimated with a QuBit fluorometer. DNA concentrations of all samples were standardized and sent to restriction-site associated DNA sequencing (RAD-Seq) in Floregenex with Illumina 4000 technology, 150bp single end, with *Pst*I as the restriction site enzyme. The overall quality of reads obtained for each species was checked with FastQC (v. 0.11.9; Babraham Bioinformatics) and data were demultiplexed with *process\_radtags* in Stacks (v. 2.60; Catchen et al., 2013) with the options set to clean the data (-c) and discard reads of low quality (-q). Demultiplexed reads can be found in the sequence read archive (SRA) database from NCBI under the numbers SAMN33770232-337 for *S. scurra*, SAMN33837911-988 for *S. variabilis*, SAMN33841405-478 for *S. ceciliana* and SAMN33841185-304 for *S. araucana*.

### 2.3 | Species identification

Morphological characteristics of the shell are inadequate to distinguish the focal species inhabiting rocky substrates due to high phenotypic variability in this trait. Therefore, we identified species following a two-step procedure. First, we used the morphological descriptions from Espoz et al. (2004) to identify and collect species from the field according to their morphological characteristics. Second, we built a molecular phylogeny by maximum likelihood based on 22,620 SNPs that included all specimens collected and morphologically assigned to the four focal species as well as specimens from other species in the genera (L. Peluso, A. Vargas, C. Asorey, S. Rosenfeld, P. Saenz-Agudelo, unpublished data). These SNPs were called de novo using Stacks, where the number of mismatches allowed within individuals and the number of mismatches allowed between individuals was set to four, and the minimum percentage of individuals across populations needed to process a locus was set to 80%. The phylogenetic analysis was made with IQtree (v. 1.6.12; Nguyen et al., 2015) using maximum likelihood, with the substitution model TVM+F based on

TABLE 1 Summary statistics of genetic diversity of the four *Scurria* species across each sample site.

	Site	N	Lat, Lon	pA	Ho	He	$\pi$	F <sub>IS</sub>
<i>S. scurra</i>	PA	12	-25.28, -70.45	1884	0.0286	0.0425	0.0445	0.0606
	CB	11	-28.09, -71.16	1955	0.0362	0.0445	0.0467	0.0386
	TE	12	-29.47, -71.31	1421	0.0356	0.0451	0.0472	0.0445
	LI	12	-30.75, -71.70	2092	0.0365	0.0458	0.0479	0.0437
	HU	12	-31.63, -71.56	1560	0.0377	0.0481	0.0503	0.0464
	PU	10	-34.06, -71.94	1237	0.0258	0.0450	0.0478	0.0745
	CN	11	-36.20, -72.95	1735	0.0440	0.0474	0.0498	0.0213
	NI	12	-39.82, -73.40	1911	0.0435	0.0469	0.0490	0.0219
	CH	12	-41.85, -74.03	1908	0.0446	0.0477	0.0498	0.0195
MA	2	-53.62, -72.30	269	0.0327	0.0264	0.0369	0.0063	
<i>S. variabilis</i>	AR	12	-18.50, -70.33	1299	0.0796	0.0863	0.0897	0.0372
	TO	14	-22.11, -70.21	1423	0.0789	0.0860	0.0889	0.0385
	PA	13	-25.28, -70.45	1235	0.0634	0.0840	0.0872	0.0869
	CB	11	-28.09, -71.16	1176	0.0688	0.0838	0.0878	0.0643
	TE	3	-29.47, -71.31	331	0.0698	0.0701	0.0853	0.0285
	LI	12	-30.75, -71.70	1305	0.0724	0.0853	0.0888	0.0599
	HU	12	-31.63, -71.56	1286	0.0740	0.0845	0.0880	0.0522
	PU	1	-34.06, -71.94	101	0.0762	0.0381	0.0758	—
<i>S. ceciliana</i>	CN	8	-36.20, -72.95	887	0.0551	0.0581	0.0618	0.0225
	NI	29	-39.82, -73.40	3334	0.0567	0.0624	0.0632	0.0486
	CH	24	-41.85, -74.03	2808	0.0567	0.0626	0.0636	0.0455
	MA	13	-53.62, -72.30	1342	0.0496	0.0563	0.0585	0.0370
<i>S. araucana</i>	AR	12	-18.50, -70.33	1144	0.0436	0.0471	0.0470	0.0213
	TO	4	-22.11, -70.21	400	0.0446	0.0435	0.0479	0.0116
	PA	12	-25.28, -70.45	964	0.0309	0.0473	0.0474	0.0682
	CB	11	-28.09, -71.16	888	0.0389	0.0476	0.0479	0.0414
	TE	15	-29.47, -71.31	1078	0.0405	0.0479	0.0475	0.0398
	LI	14	-30.75, -71.70	995	0.0401	0.0486	0.0483	0.0417
	HU	13	-31.63, -71.56	841	0.0382	0.0477	0.0476	0.0442
	PU	22	-34.06, -71.94	2141	0.0497	0.0564	0.0552	0.0456
	CN	17	-36.20, -72.95	2144	0.0531	0.0606	0.0599	0.0455

Note: For site names, see Section 2.

Abbreviations: AR, Arica; CB, Carrizal Bajo; CH, Chiloé; CN, Concepción; F<sub>IS</sub>, mean F<sub>IS</sub>; He, mean expected heterozygosity; Ho, mean observed heterozygosity; HU, Huentelauquén; LI, Limarí; MA, Magallanes; N, number of sequenced individuals; NI, Niebla; pA, number of private alleles; PA, Paposo; PU, Puertecillo; TE, Temblador; TO, Tocopilla;  $\pi$ , nucleotide diversity.

ModelFinder (Kalyaanamoorthy et al., 2017). Branch support was estimated using the ultrafast bootstrap approximation method (Hoang et al., 2018). All nodes corresponding to different species had statistical support of 100%. The species identity used here onwards corresponds to the results of this phylogeny (L. Peluso, A. Vargas, C. Asorey, S. Rosenfeld, P. Saenz-Agudelo, unpublished data).

## 2.4 | SNPs call and filtering

For *S. scurra*, *S. araucana* and *S. ceciliana* datasets, SNPs were called using the *S. scurra* genome (E. Giles, V. Gonzalez, S. Lemer, V. Suescun,

C. Leiva, C. Sartor, D. Ortiz-Barrientos, M. L. Guillemin, P. Saenz-Agudelo, unpublished data) as reference with the *ref\_map.pl* (Stacks), where individual reads were first aligned to the genome with Bowtie 2 (v. 2.4.4; Langmead & Salzberg, 2012) with end-to-end read alignment and the very sensitive option. For *S. variabilis*, SNPs were called de novo with the *denovo\_map.pl* pipeline (Stacks). We opted for this strategy because *S. variabilis* is phylogenetically distant from the other three *Scurria* species (Asorey, 2017; Espoz et al., 2004) and alignment to the *S. scurra* reference genome resulted in a very low number of markers. Hence, for the identification of *S. variabilis* the number of mismatches allowed within individuals (-M) and the number of mismatches allowed between individuals (-n) was set to four after testing with different

values following Paris et al. (2017). During SNP calling, datasets for all species were filtered by writing only the first SNP from each RAD locus and by setting 80% as the minimum percentage of individuals across populations required to process a locus in the *populations* program (Stacks). Following O'Leary et al. (2018), vcf files were further filtered for mean minimum read depth per locus (15), maximum mean depth per site (62–73, depending on the species) and a final genotype call rate of 90% with VCFtools (v. 0.1.16; Danecek et al., 2011). Individuals with 20% or more missing data were removed. The last step of data filtering consisted of removing SNPs with evidence of linkage disequilibrium (LD), which was calculated using the function *snpgdsLDpruning* from the R package *SNPRELATE* (v. 1.28.0; Zheng et al., 2012) with a 0.2 threshold. For filtering steps used in each species, see Table S1 in the Supplementary Information.

## 2.5 | Genetic diversity and structure

Summary statistics were calculated for each species' dataset to characterize their genetic diversity using *populations* from Stacks. To evaluate the genetic structure of each species, the ancestry coefficients of each individual were calculated using the sparse non-negative matrix factorization (sNMF) implemented on the R package *LEA* (v. 3.6.0; Fricot & François, 2015). The number of estimated ancestral populations ( $k$ ) ranged from 1 to 5, and 10 repetitions for each  $k$  were run. The best  $k$  was chosen based on the cross-entropy criterion and barplots were generated for the best run, that is, with the lowest cross-entropy. We used a principal component analysis (PCA) with the R package *ADEGENET* (v. 2.1.5; Jombart & Ahmed, 2011) to test for the presence of genetic clusters. To verify the distribution of genetic diversity in the genetic clusters defined in the previous analyses, we used an analysis of molecular variance (AMOVA) using the function *poppr.amova* from the R package *POPPR* (Kamvar et al., 2014) with a significance test using 999 permutations with the function *randtest.amova* from the R package *ADE4* (v. 1.7–19; Dray & Dufour, 2007).

## 2.6 | Isolation by distance

To test if the genetic differentiation found was associated with geographical distance, that is, if genetic differentiation followed a pattern of isolation by distance (IBD), we used a Mantel test using  $F_{ST}$  and the linear geographic distance between sites with the *mantel* function in the *vegan* R package with 999 permutations to test for significance (v. 2.5–7; Oksanen et al., 2020).  $F_{ST}$  was calculated in *HIERFSTAT* (Goudet & Jombart, 2021) and geographic distance with *geosphere* R package (v. 1.5–14; Hijmans, 2021).

## 2.7 | Outlier loci

Another factor that can affect the estimated genetic structure is the occurrence of outlier loci, that is, loci with differentiation patterns

that deviate from neutrality and that may be associated with selection. We used two analyses to identify the presence of loci that deviated from neutrality. The first test was based on allele frequencies among populations and was implemented in *BAYESCAN* (v. 2.1; Foll & Gaggiotti, 2008), where the parameters were a threshold  $q$ -value < 0.05 and prior odds for the neutral model equal to 100. The second analysis was based on individual genotypes and was implemented using the R package *PCADAPT* (v. 4.3.3; Privé et al., 2020) and with outliers defined as the top 1% quantile of  $p$ -values. Genetic structure analyses (sNMF and PCA) were performed using datasets including only the outliers separately to test for differences in genetic structure between neutral loci and these putative loci under selection.

## 2.8 | Demographic history

Present genetic diversity and structure estimates can be affected by historical fluctuations in population size and migration events. We estimated the demographic history of our study species using a modified diffusion approximation of the Wright–Fisher population model implemented in the software *GADMA* (Noskova et al., 2020). *GADMA* infers the joint demographic history of up to three populations from genetic data and has the advantage over other programs of implementing a genetic algorithm (GA) to explore models and parameter space based on the principle of 'natural selection'. The GA works by initially generating a random set of models following the user instructions, and then mutating these models by random changes of parameter values or crossing over parameters from different models randomly as well. The algorithm tracks the 'fitness' of these changes and keeps only those for which a significant improvement of data fitting is observed. This software uses two known engines for demographic inference, *∂a∂i* (Gutenkunst et al., 2010) and *moments* (Jouganous et al., 2017). Here, we used *moments* as previous studies have shown it produces robust results and is more computationally efficient (Noskova et al., 2020). Outlier loci detected by both methods were removed from the datasets for this analysis. Species' datasets were reduced to include only one site (i.e. one geographic location) for each population defined in the genetic structure analyses to avoid problems with substructure. Sites with less missing data per individual and higher number of samples were selected. The program requires the user to define the order in which the populations split when three populations are modelled. To define this, we used phylogenetic trees reconstructed using maximum likelihood with the program *IQ-TREE* to choose the most ancient population: the population sister to the remaining populations in the phylogeny or more closely related to the outgroup (other *Scurria* species). Because our small sample sizes could introduce noise to the estimated allele frequency spectrum, we allowed only one size change per time period to decrease the number of parameters in our models, thus avoiding model overfitting (Noskova et al., 2020). We also restricted our models to sudden population changes only for the same reasons. For each model run the initial and final structures were set to [1,1] or

[1,1,1] depending on the number of populations detected with the genetic data. The local search algorithm optimization was the BFGS method with log transformation. Parameter search and optimization was repeated 10 times for each model. Sequence length was set for each species depending on the number of total RAD loci found and we retained loci as described in GADMA documentation (<https://gadma.readthedocs.io/>). The average genomic mutation rate for the *Scurria* group remains unknown, so we used a mutation rate of  $1.7e-9$  based on a recent publication that estimated the nuclear mutation rate for other molluscs (Allio et al., 2017). For each species, a model with and another without migrations was tested, maintaining all other parameters equal. Parameters for the GA were left as default as recommended by developers (for details see Noskova et al., 2020). Finally, we compared and ranked the models using the Akaike Information Criterion (AIC).

### 3 | RESULTS

#### 3.1 | Species identification

Genetic identification revealed substantial differences with morphological identification for *Scurria variabilis*, *Scurria cecilians* and *Scurria araucana*. While these differences were not the aim of this study, it is important to note that genetic species assignments revealed overwhelming phenotypic variability in shell morphology among species. It also indicated clear and previously unknown latitudinal segregation, where *S. variabilis* was only observed in sites north of  $34^{\circ}\text{S}$ ,

*S. araucana* was found only north of  $36^{\circ}\text{S}$  and *S. cecilians* was only found in sites south of  $36^{\circ}\text{S}$  (Figure 1).

#### 3.2 | Assembly statistics and genetic diversity

We mapped to the reference genome a total of 58,770 RAD loci for *S. scurra*, 45,251 variant sites remained after SNP call, and after additional filters we kept 28,124 SNPs. For *S. variabilis*, we assembled 29,585 RAD loci, 29,345 variant sites remained after SNP call and we kept 16,733 SNPs after further filtering steps. For *S. cecilians*, we mapped to the reference genome 36,673 RAD loci, 27,756 variant sites remained after SNP call and we kept 13,451 SNPs after filtering. Finally, for *S. araucana* we mapped to the reference genome 44,032 RAD loci, 33,718 variant sites remained after SNP call and 21,158 SNPs were retained after filtering. The number of individuals sampled for each species from each site and summary statistics are given in Table 1. The species with the highest values of nucleotide diversity ( $\pi$ ), and observed and expected heterozygosity was *S. variabilis* (Table 1). The values of  $\pi$  across latitude were somewhat homogeneous for all species except for *S. araucana*, with higher diversity observed in two central-southern sites (PU and CN) (Figure 2a). For *S. cecilians* and *S. scurra* the southernmost site (MA) had the lowest value of  $\pi$ , in the case of *S. scurra* likely associated with low sample size ( $N=2$ ; Table 1). The inbreeding coefficient  $F_{IS}$  showed a more heterogeneous latitudinal variation, with relatively higher  $F_{IS}$  values in central sites where most species overlap (Figure 2b). Besides, a peak of high  $F_{IS}$  values was found in

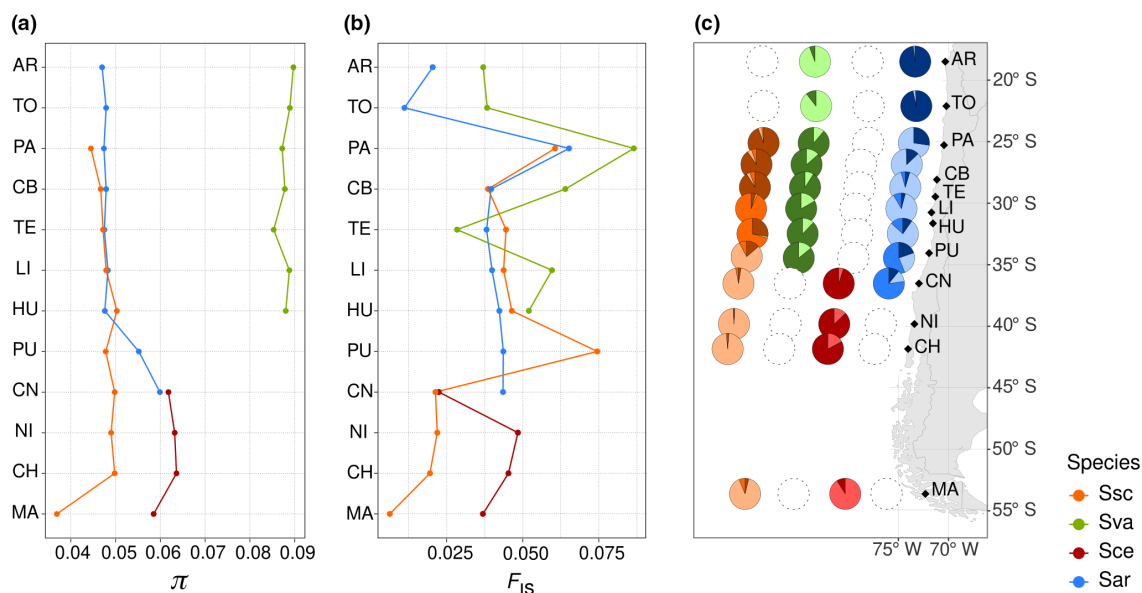


**FIGURE 2** Plots and maps showing the results by sampling site for each species. The estimated values of nucleotide diversity ( $\pi$ ) (a), Inbreeding coefficient ( $F_{IS}$ ) (b) and the mean admixture proportions (c) are given. The circle charts correspond to the allele frequency proportion estimated by the sNMF analyses for  $k=3$  for *Scurria scurra* (Ssc),  $k=2$  for *Scurria variabilis* (Sva),  $k=2$  for *Scurria cecilians* (Sce) and  $k=3$  for *Scurria araucana* (Sar). Empty circles correspond to sites where no individuals from that species were identified. For site names, see Section 2. AR, Arica; CB, Carrizal Bajo; CH, Chiloé; CN, Concepción; HU, Huentelauquén; LI, Limarí; MA, Magallanes; NI, Niebla; PA, Paposos; PU, Puertecillo; TE, Temblador; TO, Tocopilla.

the northern PA site for the species recorded at the site: *S. scurra*, *S. variabilis* and *S. araucana* (Figure 2b). The matches of high  $F_{IS}$  overlapped with a genetic break for the latter two (described below) and the northern distribution limit for *S. scurra*. Another high  $F_{IS}$  peak observed for *S. scurra* in PU also coincided with one of the genetic breaks described for this species.

### 3.3 | Genetic structure

The spatial distribution of genetic structure varied among species but there were also several similarities. For *S. scurra*, the best  $k$  estimated by sNMF was four (Figure S1), but inspection of the associated barplot reveals three groups with the fourth population corresponding to only a few individuals (two from TE, two from HU) (Figure 3a). Results from PCA corroborated the distribution of samples in these three groups (Figure 3a). The northern group consisted of three sites north of 30°S latitude (TE, CB and PA), the central group was bounded between 30°S and 34°S and comprised two sites (LI, HU), although we note that some individuals found there displayed clear ancestry from the northern group. The southern group included all

sites from 34°S to 54°S. For *S. variabilis*, the best estimated  $k=1$  (Figure S1), however, the barplots from  $k \geq 2$  show that the northern sites AR and TO are grouped and separated from the rest of the samples (Figure 3b). This was supported by the PCA where samples from AR and TO sites were separated from the rest (Figure 3b). For *S. cecilians*, the best  $k$  was also 1 (Figure S1), but samples from the southernmost site (MA) separated when  $k \geq 2$  (Figure 3c). The PCA for *S. cecilians* showed that indeed samples from MA clustered together and were slightly separated from the other sites (Figure 3c). In the case of *S. araucana*, the best estimated  $k$  was 2 (Figure S1) where the central-southern sites PU and CN are separated from the others (Figure 3d). Inspection of the barplots for  $k \geq 2$  showed that besides these sites, AR and TO also appeared as a distinct cluster, which was also evidenced in the PCA, where samples were sorted following their geographic distance (Figure 3d). The results from AMOVA indicated that the majority of variation was observed between samples and within individuals for all species (Table 2). For *S. cecilians*, we did not calculate variation between genetic groups given that one group consisted of only samples from one site (MA). Variation between genetic groups explained a considerable amount of variation for *S. scurra* (11%) and in a lower proportion for *S. araucana* and

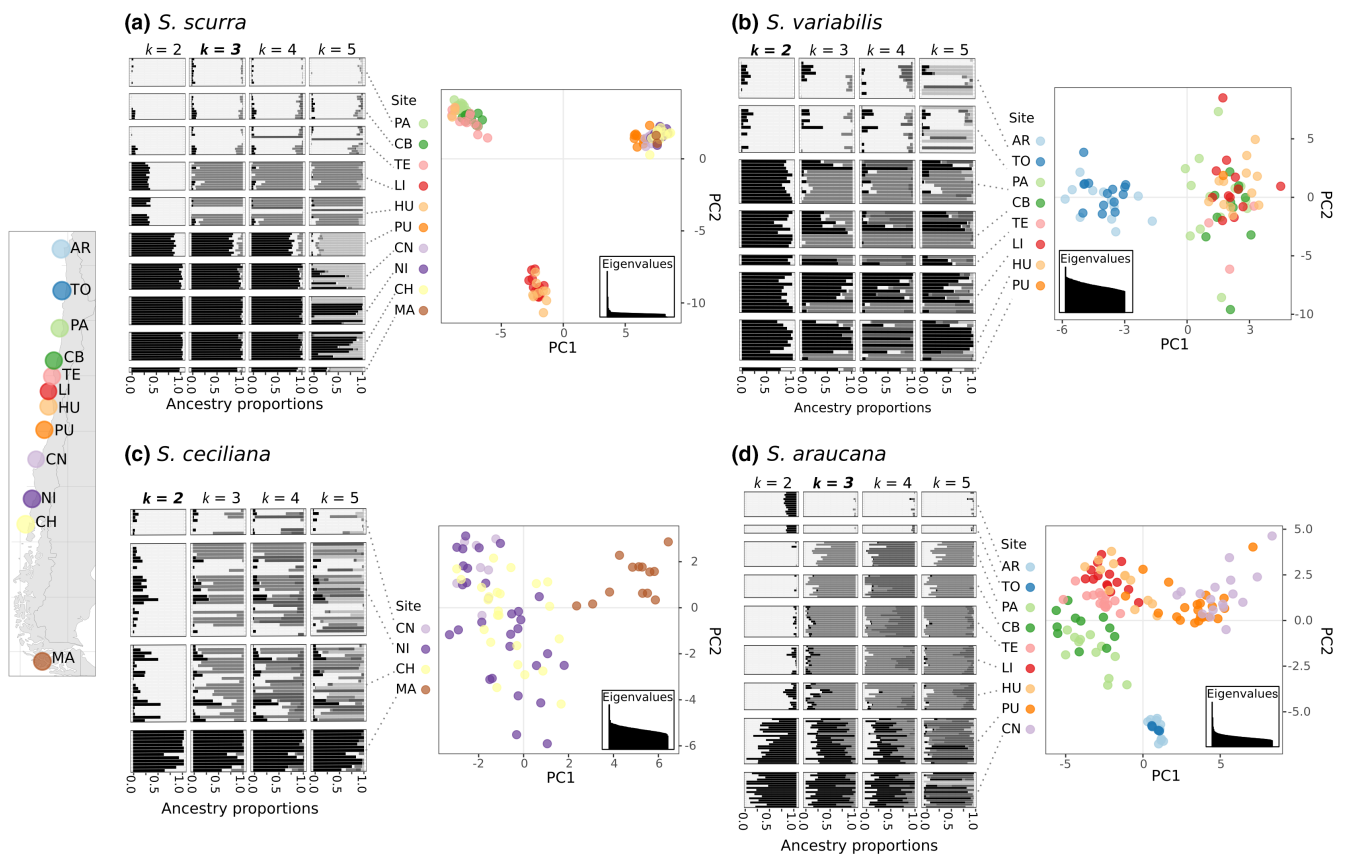


**FIGURE 3** Barplots showing the ancestry proportions of each individual (bars) from the sNMF analyses for  $k=2$  to  $k=5$  and plots showing the first two principal components from the PCA for *Scurria scurra* (a), *Scurria variabilis* (b), *Scurria cecilians* (c) and *Scurria araucana* (d) for the datasets with all filtered SNPs (neutral and outlier). Favoured  $k$  number for each species is highlighted in bold and italics. For site names, see Section 2. AR, Arica; CB, Carrizal Bajo; CH, Chiloé; CN, Concepción; HU, Huentelauquén; LI, Limarí; MA, Magallanes; NI, Niebla; PA, Paposos; PU, Puertecillo; TE, Temblador; TO, Tocopilla.

	<i>Scurria scurra</i>	<i>Scurria variabilis</i>	<i>Scurria cecilians</i>	<i>Scurria araucana</i>
Between groups	11.81	1.07	—	3.17
Between sites within groups	1.55	0.09	0.99	0.88
Between samples within sites	17.55	13.48	8.34	14.21
Within samples	69.09	85.36	90.67	81.73

Note: For *S. cecilians*, variance between groups was not calculated considering that one group only included one sampling site.

*S. variabilis* (Table 2). The variation between sites within groups was low and accounted for ~1% of the total variation explained for all four species (Table 2).

### 3.4 | Isolation by distance

The Mantel tests showed a significant correlation between genetic and geographic distance for all species; the relationship was weaker in *S. variabilis* and stronger for *S. scurra* as observed by the difference between the slopes (Figure 4). For *S. variabilis* the PU site was removed considering it only had one sample and for *S. scurra* the MA site was removed since it consisted of only two samples at the extreme of the geographic gradient examined. The mantel correlation was higher for *S. cecilians* ( $R = .96$ ,  $p = .042$ ), followed by *S. araucana* ( $R = .85$ ,  $p = .001$ ), *S. variabilis* ( $R = .75$ ,  $p = .011$ ) and finally *S. scurra* ( $R = .67$ ,  $p = .002$ ).

### 3.5 | Outlier loci

The number of common loci detected by both outlier analyses was 35 for *S. scurra*, eight for *S. variabilis*, 10 for *S. cecilians* and 27 for *S. araucana* (Table S2). None of these outliers were common among *S. scurra*, *S. cecilians* and *S. araucana* when we looked at the genomic distribution of the outlier loci along the *S. scurra* reference genome. The closest distance between two outlier loci from different species was 27 Kb. However, two linkage groups harboured most of the outlier loci and shared outlier loci for two or three species (LG3: 17 loci for *S. araucana*, five for *S. scurra*; LG466: eight for *S. cecilians*, four for *S. scurra* and five for *S. araucana*; Figure S2). Major allele frequency distributions across sampling sites for outlier loci for the two sympatric species, *S. araucana* and *S. scurra*, revealed important differences. For *S. scurra*, all loci had one allele that is near fixation south of PU, while for *S. araucana*, allele frequency changes are less drastic (Figure S3). The genetic structure results for the datasets with only the outliers and those without the outliers were almost identical and followed the structure pattern described above (Figures S4–S7).

### 3.6 | Demographic history

The demographic history analyses for all species showed that models that included migration provided a better fit, with smaller AIC values

TABLE 2 Results of the AMOVA showing the percentage of variance in each stratification, with the groups defined by genetic analyses (groups) and the sampling sites (sites).

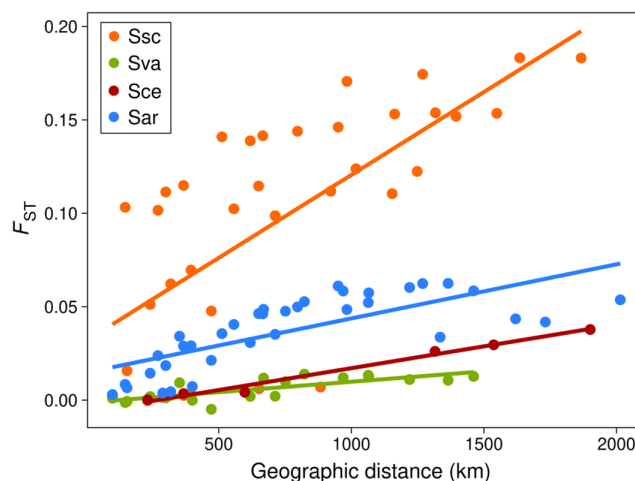
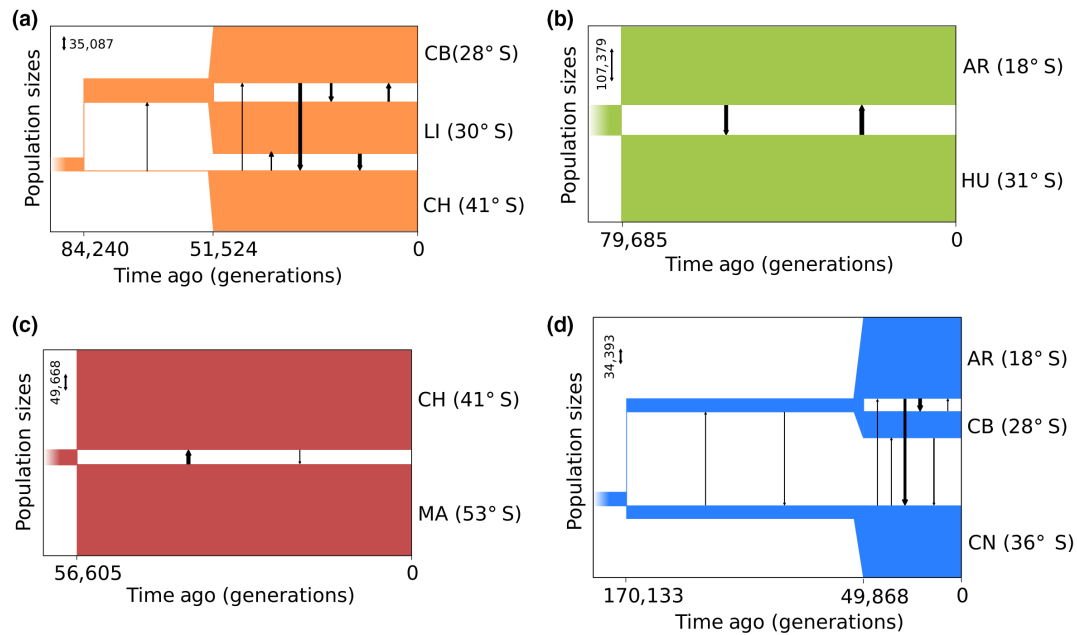


FIGURE 4 Plot showing the Mantel correlation between genetic distance ( $F_{ST}$ ) and geographic distance (km) among sites for *Scurria scurra* (Ssc), *Scurria variabilis* (Sva), *Scurria cecilians* (Sce) and *Scurria araucana* (Sar).

than models without migration (Table S3). The observed allele frequency spectrum, the expected frequency spectrum, the residuals and the histogram of residuals of the selected model are given in Figure S8. All species showed signs of recent population expansion (Figure 5). For *S. scurra*, the CB, LI and CH sites were used as representatives of each of the three populations previously described, and the southernmost (CH) was used as the most ancient population given the basal position of samples from this site in relation to the others in the phylogenetic tree (data not shown). The best demographic model indicated that there was only northward migration after the first split separating southern and northern sites, but after the second split, migration was mainly to the south (from LI and CB to CH; Figure 5a). Although after the second split all populations show an increase in size, the southernmost population (CH) shows a bottleneck pattern with a drastic population contraction during the period between the first and second population splits (Figure 5a). In the model for *S. variabilis*, the AR and HU sites were used as representatives of the populations previously detected. The best demographic model indicated an increase in size for both populations after they split and high migration in both directions, corroborating their low genetic divergence (Figure 5b). The models of demographic history for *S. cecilians* included MA and CH sites as representatives of the two predefined populations. The best model indicates an expansion in size for both populations and a prevalence of migration to the north (from MA to CH; Figure 5c). In the



**FIGURE 5** Best model of demographic history estimated by GADMA for *Scurria scurra* (a), *Scurria variabilis* (b), *Scurria ceciliana* (c) and *Scurria araucana* (d). Horizontal bars show population size variations with time and the timing of population splits. Arrows indicate migration direction and intensity in each time period.

demographic models for *S. araucana*, we used the AR, CB and CN sites as sample populations. Considering the phylogeny for this species was comb-like and could not resolve the, models were run alternating the most ancient population and the model with the southernmost site (CN) was selected based on the lower AIC (Table S2). The best model shows that migration occurred after the first split and intensified after the second split, with the northernmost site (AR) being the most common source for the other two populations (Figure 5d). In this species, all populations suffered bottlenecks and population reduction was similar (Figure 5d). Finally, comparing the best models for all four species indicates certain congruences in terms of the times of divergence, in particular, all models include one population split around 50,000–70,000 generations ago.

#### 4 | DISCUSSION

Our results show that for the four *Scurria* species analysed here, genetic diversity is spatially structured and geographically concordant among pairs of species with sympatric distributions. The strength of population genetic structure varied among species, with *S. variabilis* showing the weakest genetic structure and *S. scurra* the strongest. Two common genetic breaks were observed, one shared by *S. araucana* and *S. variabilis* at 22–25°S and the second shared by *S. araucana*, *S. scurra* and other coastal invertebrates at 31–34°S. *Scurria scurra* is the species with the narrowest microhabitat, the stipe and holdfasts of kelps, an ecological characteristic that could explain the marked genetic differentiation we found here. In addition, all species displayed signatures of divergent selection and showed signs of population expansions following population splits around similar

times (50,000–70,000 generations ago). These results suggest that oceanographic features in the region act as soft barriers for some species and that historical climate stability is associated with population diversification and expansion in these limpets. Below, we discuss how these results shed light on the common evolutionary processes that can be associated with the genetic patterns observed, and provide perspectives for further work that will help dissect the contribution of oceanographic, environmental and geographic factors to the distribution of genetic diversity in these organisms.

Common genetic breaks among congeneric species have been observed for other limpets, such as *Cellana* from New Zealand and Hawaii (Bird et al., 2007; Goldstien et al., 2006). Such coincidence was attributed to shared historical and contemporary oceanographic processes shaping gene flow, which could also be the case of the patterns observed here for *Scurria*. The first shared genetic break was observed for *S. araucana* and *S. variabilis* between 22 and 25°S (TO and PA sites), also corresponding to the northern edge of *S. scurra*'s range (Figure 1) and a genetic discontinuity previously reported for *Scurria viridula* (Saenz-Agudelo et al., 2022). Since this area coincides with the major upwelling centre at Mejillones Peninsula (~23°S; Letelier et al., 2012), the oceanographic variations caused by upwelling could act as a barrier to dispersal for larvae. The second shared break occurs within the Intermediate Area (IA), but not at the more obvious location at 30°S that is thought as an important limit, being associated with the distribution limit of many species and changes in upwelling seasonality patterns (Camus, 2001; Thiel et al., 2007). This region at 30°S is also one of the major upwelling centres in Chile, located around Lengua de Vaca Peninsula (Aguirre et al., 2012), and genetic breaks associated with it were observed for some invertebrates, such as the barnacle

*Notochthamalus scabrosus*, the gastropod *Tegula atra* and the amphipod *Orchestoidea tuberculata* (Haye et al., 2014; Zakas et al., 2009). However, for the limpets studied here only *S. scurra* had a break in this region between 29 and 30°S (TE and LI sites). The shared break occurs further south in the IA for *S. scurra* and *S. araucana*, between 31 and 34°S (HU and PU sites, Figure 2c). This second shared break is also common to *Scurria zebrina* and other invertebrates, such as the gastropod *Acanthina monodon*, the tunicate *Pyura chilensis*, the beach-dwelling brooder *Excirrolana hirsuticauda* and the barnacle *Notochthamalus scabrosus* (Barahona et al., 2019; Haye et al., 2019; Quesada-Calderón et al., 2021; Saenz-Agudelo et al., 2022; Sánchez et al., 2011). A previous study also estimated a genetic break around 30°S for *S. scurra*, but it did not have the spatial resolution to separate it from the break at 31–34°S (Haye et al., 2014). In fact, many population genetic studies on the Chilean coast have focused on large-scale phylogeographic questions, thus using a low spatial resolution that can hamper the distinction between this limit at 30°S and the previously discussed limit at 31–34°S. Taken together, our results indicate that the region comprised between 29° and 35°S harbours at least two places where genetic transitions occur for more than a single species. Some of the environmental and oceanographic settings that might be responsible for this are discussed below, but clearly, more comparative population genomic studies with more intensive sampling in the regions are warranted to better understand the evolutionary processes responsible for these common patterns that start to emerge.

The genetic limits reported above occur within either major upwelling centres or regions of complex oceanography that could act as barriers to dispersal in *Scurria* limpets. Nearshore upwelling circulation is locally intensified around large capes and headlands and slowed on bays on the lee of such topographic features (Largier, 2020). In this way, the interaction between coastal geomorphology, wind and coastal circulation can maintain persistent spatial structure in the larval delivery over large spatial scales (Broitman et al., 2008; Navarrete et al., 2005). Intensification around upwelling centres can increase offshore transport in the surface layer, advecting larvae away from their adult benthic habitat; onshore transport can take place in deeper layers or during relaxation from upwelling, while larvae may be retained in bays (Largier, 2020; Roughan et al., 2005). In addition, upwelling waters along the Southeastern Pacific Ocean are characterized by low oxygen concentrations, low pH and elevated  $p\text{CO}_2$ , which represents challenging conditions for the larvae and juveniles of calcifying organisms (Hettinger et al., 2013; Ramajo et al., 2020; Vargas et al., 2020). For broadly distributed species such as *Scurria*, such environmental variations can lead to populations differences in population dynamics (Broitman et al., 2001; Navarrete et al., 2008; Rivadeneira et al., 2002) and phenotypic response (Broitman et al., 2021; Lardies et al., 2021; Ragonieri et al., 2009; Rodríguez-Romero et al., 2022). Considering this might also reflect differences in dispersal and recruitment, such upwelling centres can act as soft barriers by hampering dispersal and lead to the genetic discontinuities observed in 22–25°S and 29–30°S. Indeed, one study has shown that there is a change in recruitment patterns across the

major upwelling centre of Lengua de Vaca Peninsula, where recruitment rates were higher north of this upwelling (Valdivia et al., 2015), which indicates the effect of the upwelling in species dispersal. The second shared genetic break at 31–34°S occurs further south of a major upwelling centre and comprises a region characterized by intense oceanographic variability at the mesoscale and marks the area where riverine inputs become progressively more important poleward (Lara et al., 2019; Saldías et al., 2016). Although no specific oceanographic feature can be associated with this limit, it shows that the coast of central Chile is more heterogeneous than previously thought and that higher spatial resolution in future studies coupled with biophysical models that can simulate larval dispersal (Swearer et al., 2019) should provide a better understanding of connectivity patterns in the region between 30° and 35°S and what evolutionary processes have shaped them.

Two analysed *Scurria* occur in the Magellanic region, thus crossing the biogeographic limit at 42°S. Interestingly, for *S. scurra* no structure is observed between Magallanes (MA) and Chiloé (CH), two sites that are more than 10° of latitude apart (but this could be a consequence of our low N in MA, see Table 1), while two breaks are observed within the IA in 5° of latitude. Although the breaks along the central-northern region could be associated with the persistent mesoscale environmental structure discussed above, the spatial pattern can also be related to the different kelp species that host *S. scurra* between regions. North of 30°S the only kelp in the rocky intertidal zone is *Lessonia berteroa*, which is replaced by *Lessonia spicata* and *Durvillaea incurvata* south of the 30°S break and joined by *Durvillaea antarctica* south of the 42°S biogeographic break (Fraser et al., 2020; González et al., 2012). In the south, having *Durvillaea* spp. as hosts likely increased *S. scurra* population size and dispersal potential due to rafting since these limpets can usually be found on stranded algae (López et al., 2018). *Durvillaea* kelps are highly buoyant, being able to disperse for hundreds to thousands of kilometres (Fraser et al., 2011, 2018), and the associated high dispersal could account for the high gene flow observed in *S. scurra* in the Magellanic region. On the other hand, for *S. ceciliania* a genetic break was present between 41 and 53°S (CH and MA sites). The limit between the IA and the Magellanic Province around 41–43°S is a region that marks a contrasting shift in geological features, ocean currents and the influence of historical glaciations (Camus, 2001; Pantoja et al., 2011). Genetic breaks around this region were also observed in other invertebrates, such as the barnacle *Notochthamalus scabrosus* and the mussel *Perumytilus purpuratus*, although displaced north (40°S; Ewers-Saucedo et al., 2016; Guíñez et al., 2016). It would be interesting to know the exact location of the genetic break between *S. ceciliania* populations since it may not correspond to the biogeographic limit. The area between 42 and 54°S is an irregular insular system that imposes major logistic constraints for sampling, which explains the sparse locations sampled here and in previous studies across the region (e.g. Ewers-Saucedo et al., 2016; Guíñez et al., 2016; Sánchez et al., 2011). While future population genetic studies for benthic populations in the central-northern coast should employ spatially intensive sampling around known breaks, studies

around the southern region should aim to cover the vast areas where no specimens have ever been collected in order to reveal the existence of undetected breaks.

The demographic histories estimated here indicated a common population divergence followed by demographic expansion for all species around 50,000–70,000 generations ago. For all species the best model involved isolation with migration after population divergence. We can only speculate about the age of population splits since estimates are based on a rough approximation of the mutation rate and an assumption of generation time of 1 year. The timing of divergence is intriguing since it could coincide with an early warm period (51–61 Ka) according to current palaeoclimatic reconstruction (Kaiser et al., 2005). Our data are insufficient to be confident about the estimated time of divergence in years, but the coincidence of these divergences and population expansion timing among species suggests they happened in similar time periods in the past, thus could be linked to similar climatic conditions. Interestingly, the most ancient split inferred for both *S. araucana* and *S. scurra* occurred between populations from north and south of  $\sim 30^\circ\text{S}$ , suggesting this area corresponds to a transition zone preceding this last population split. This concordance shows that the common genetic break observed in these species might be associated with common historical isolation rather than a modern barrier to dispersal caused by oceanographic conditions, or it might be that both processes act together to maintain this genetic limit in these species. Additionally, the majority of outlier loci of *S. scurra* and *S. araucana* were located in two linkage groups and some were quite close to each other, showing also a marked change in allele frequency in the region, specifically in the transition from the HU to PU sites (Figures S2 and S3). Considering these two linkage groups are different from the one reported for *S. zebrina* at the same geographic transition (Saenz-Agudelo et al., 2022), these results suggest there are similar adaptation responses in these two sister limpets although not in the same genes. Despite the more severe population reduction observed in *S. scurra*, the southernmost population of *S. araucana* showed higher levels of inbreeding, indicating important differences in the isolation process of these populations, such as in recolonization patterns and refugia availability (Alcala & Vuilleumier, 2014). Thus, different mechanisms at the molecular level could be associated with selection acting on similar traits related to these historical environmental changes in the central-southern region, but further studies are needed to test this idea.

The differences in genetic breaks reported here can also be due to other factors besides barriers or historical demographic changes, such as differences in life-history traits related to population dynamics, for example, pelagic larval duration, reproductive output or population sizes (Dawson et al., 2014). Unfortunately, to our knowledge, almost no available published data concerning *Scurria* larval characteristics is available. Only one work has reported the timing and mode of reproduction of *S. scurra* in one locality in southern Chile (Río Cardoza, 1992). However, for many patellogastropods pelagic larval duration (PLD) has been measured and appears relatively conserved, with pre-settlement period ranging from 3 to 7 days and

pelagic larval duration around 10 days (Kay & Emler, 2002; Kolbin & Kulikova, 2011; Kuo & Sanford, 2013; Page, 2002). Therefore, it is reasonable to assume that PLD for *Scurria* would be within this range. Concerning species population sizes, one study has reported the abundances of several *Scurria* across their geographic ranges and showed no intraspecific differences between central and peripheral populations (Espoz, 2002). However, the same study showed significant differences in abundance among *Scurria* species, *S. ceciliansa* showed the highest abundances, followed by *S. scurra*, *S. variabilis* and *S. araucana* (Espoz, 2002). These differences suggest that effective population sizes are different among species, and somehow correlate with what we report here in terms of genetic diversity estimates and genetic structure. Yet, it is important to take into account that our data indicate that at least three species (*S. ceciliansa*, *S. araucana* and *S. variabilis*) display enormous variation in shell morphology, which has probably led to the misidentification of specimens in the past. Thus, further studies to quantify species abundance along the Chilean coast are required to further evaluate if population sizes are a significant factor that explains differences in genetic structure among species. Another factor that could explain the genetic patterns could be associated with changes in larval development, and thus, pelagic larval duration as a function of water temperature. A study with the patellogastropod *Lottia digitalis* showed that larval development took twice as long when larvae were reared in  $8^\circ\text{C}$  when compared to the larvae at  $13^\circ\text{C}$  (Kay & Emler, 2002). If this pattern is similar in *Scurria* and in natural populations, then we could assume that larvae should disperse for longer periods and longer distances in the south, compared to the north. This, in turn, would explain the higher genetic differentiation in northern-central sites for *S. scurra*, *S. variabilis* and *S. araucana*. Interestingly, migration estimates suggest asymmetric gene flow for three species, with major migration going southwards for *S. scurra* and *S. araucana*, and most migration going northwards for *S. ceciliansa*. Our results suggest that net migration for these species is in the opposite direction of the two main oceanographic currents (Strub et al., 2019). In this region, the South Pacific Current approaches Chile from the east between  $40^\circ$  and  $50^\circ\text{S}$  and bifurcates into the Humboldt Current that flows northward and the Cape Horn Current that flows southwards. Altogether, further studies that characterize *Scurria* larval development and behaviour could greatly improve our understanding of their connectivity and migration patterns, clarifying what different processes cause them.

Overall, our results clearly show that the four analysed *Scurria* species share some common patterns of genetic structure and demographic histories. This is expected considering that they share similar habitats and reinforce the notion that common contemporary and historical environmental processes shape ecology and evolution. These results highlight how comparative studies with congeneric species with similar life-history traits can help uncover important processes in the landscape that impede gene flow and that might be associated with adaptations. Besides, understanding common historical demographic changes also allows for inferring ancient processes, in this case likely associated with historical habitat availability

and conditions, that lead to genetic divergence in some populations and show the common influence of climate stability in species that live in the same habitat. Although specific breaks and genetic diversity patterns were observed here, the common features indicate how similar ecological restraints can shape similar evolutionary outcomes. Clearly, further studies will be needed to better understand the oceanographic and environmental complexity of the area and how different drivers are shaping genetic diversity. Finally, this study showed how shared and specific patterns of genetic connectivity coexist in a region among endemic and sympatric species, evidencing how comparative studies help identify the common evolutionary processes that shape species genetic differentiation and that, ultimately, contribute to the marine biodiversity patterns in a given seascape.

#### AUTHOR CONTRIBUTIONS

Conceptualization: L.P., B.R.B., M.A.L., R.N. and P.S.-A. Designed research: L.P. and P.S.-A. Performed research: L.P. and P.S.-A. Contributed new reagents or analytical tools: L.P., B.R.B., M.A.L., R.N. and P.S.-A. Analysed data: L.P. and P.S.-A. Writing—original draft: L.P. Writing—review and editing: B.R.B., M.A.L., R.N. and P.S.-A.

#### ACKNOWLEDGEMENTS

We acknowledge the support from Fondo Nacional de Desarrollo Científico y Tecnológico (FONDECYT 1190710) and L.P. acknowledges the doctoral scholarship from ANID (21170187). We thank Felipe Pontigo, Paula Ramirez, Alejandra Vargas and members of the Saenz and Chango labs for assistance in the field and in the laboratory.

#### CONFLICT OF INTEREST STATEMENT

The authors declare no conflict of interests.

#### DATA AVAILABILITY STATEMENT

Individual fastq data files are available at the SRA repository of NCBI under BioProject number PRJNA944965. The VCF files containing all SNPs loci after filtering steps, all SNPs except the putative outlier loci and only the putative outlier loci for each species can be found at <https://doi.org/10.5061/dryad.k98sf7mbs>.

#### ORCID

Livia Peluso  <https://orcid.org/0000-0002-6365-5392>

Bernardo R. Broitman  <https://orcid.org/0000-0001-6582-3188>

Marco A. Lardies  <https://orcid.org/0000-0003-3525-1830>

Roberto F. Nespolo  <https://orcid.org/0000-0003-0825-9618>

Pablo Saenz-Agudelo  <https://orcid.org/0000-0001-8197-2861>

#### REFERENCES

- Aguirre, C., Pizarro, Ó., Strub, P. T., Garreaud, R., & Barth, J. A. (2012). Seasonal dynamics of the near-surface alongshore flow off Central Chile. *Journal of Geophysical Research: Oceans*, 117(1), 1–17.
- Alcala, N., & Vuilleumier, S. (2014). Turnover and accumulation of genetic diversity across large time-scale cycles of isolation and connection of populations. *Proceedings of the Royal Society B: Biological Sciences*, 281(1794), 20141369.
- Allio, R., Donega, S., Galtier, N., & Nabholz, B. (2017). Large variation in the ratio of mitochondrial to nuclear mutation rate across animals: Implications for genetic diversity and the use of mitochondrial DNA as a molecular marker. *Molecular Biology and Evolution*, 34(11), 2762–2772.
- Asorey, C. M. (2017). *Diversificación y coexistencia de Lottidae (Mollusca: Patellogastropoda) en la costa del Pacífico Suroriental*. [PhD thesis, Facultad de Ciencias del Mar, Universidad Católica].
- Barahona, M., Broitman, B. R., Faugeron, S., Jaugeon, L., Ospina-Alvarez, A., Véliz, D., & Navarrete, S. A. (2019). Environmental and demographic factors influence the spatial genetic structure of an intertidal barnacle in Central-Northern Chile. *Marine Ecology Progress Series*, 612, 151–165.
- Bird, C. E., Holland, B. S., Bowen, B. W., & Toonen, R. J. (2007). Contrasting phylogeography in three endemic Hawaiian limpets (*Cellana* spp.) with similar life histories. *Molecular Ecology*, 16(15), 3173–3186.
- Bowen, B. W., Gaither, M. R., DiBattista, J. D., Iacchi, M., Andrews, K. R., Grant, W. S., Toonen, R. J., & Briggs, J. C. (2016). Comparative phylogeography of the ocean planet. *Proceedings of the National Academy of Sciences of the United States of America*, 113(29), 7962–7969.
- Brattström, H., & Johannsen, A. (1983). Ecological and regional zoogeography of the marine benthic fauna of Chile. *Sarsia*, 68(4), 289–339.
- Broitman, B., Navarrete, S., Smith, F., & Gaines, S. (2001). Geographic variation of southeastern pacific intertidal communities. *Marine Ecology Progress Series*, 224, 21–34.
- Broitman, B. R., Blanchette, C. A., Menge, B. A., Lubchenco, J., Krenz, C., Foley, M., Raimondi, P. T., Lohse, D., & Gaines, S. D. (2008). Spatial and temporal patterns of invertebrate recruitment along the west coast of the United States. *Ecological Monographs*, 78(3), 403–421.
- Broitman, B. R., Lagos, N. A., Opitz, T., Figueroa, D., Maldonado, K., Ricote, N., & Lardies, M. A. (2021). Phenotypic plasticity is not a cline: Thermal physiology of an intertidal barnacle over 20° of latitude. *Journal of Animal Ecology*, 90(8), 1961–1972.
- Camus, P. A. (2001). Biogeografía marina de Chile continental. *Revista Chilena de Historia Natural*, 74(3), 587–617.
- Cárdenas, L., Castilla, J. C., & Viard, F. (2009). A phylogeographical analysis across three biogeographical provinces of the South-Eastern Pacific: The case of the marine gastropod *Concholepa concholepa*. *Journal of Biogeography*, 36(5), 969–981.
- Catchen, J., Hohenlohe, P. A., Bassham, S., Amores, A., & Cresko, W. A. (2013). Stacks: An analysis tool set for population genomics. *Molecular Ecology*, 22(11), 3124–3140.
- Danecek, P., Auton, A., Abecasis, G., Albers, C. A., Banks, E., DePristo, M. A., Handsaker, R. E., Lunter, G., Marth, G. T., Sherry, S. T., McVean, G., Durbin, R., & 1000 Genomes Project Analysis Group. (2011). The variant call format and VCFtools. *Bioinformatics*, 27(15), 2156–2158.
- Dawson, M. N., Hays, C. G., Grosberg, R. K., & Raimondi, P. T. (2014). Dispersal potential and population genetic structure in the marine intertidal of the eastern North Pacific. *Ecological Monographs*, 84(3), 435–456.
- Dray, S., & Dufour, A. (2007). The ade4 package: Implementing the duality diagram for ecologists. *Journal of Statistical Software*, 22(4), 1–20.
- Espoz, C. (2002). *Relaciones ecológicas y evolutivas entre los patelogastrópodos intermareales endémicos a la costa rocosa de Perú y Chile: Distribución, abundancia y filogenia*. [PhD thesis, Pontificia Universidad Católica de Chile, Chile, 253 p].
- Espoz, C., Lindberg, D. R., Castilla, J. C., & Simison, W. B. (2004). Los patelogastrópodos intermareales de Chile y Perú. *Revista Chilena de Historia Natural*, 77(2), 257–283.
- Ewers-Saucedo, C., Pringle, J. M., Sepúlveda, H. H., Byers, J. E., Navarrete, S. A., & Wares, J. P. (2016). The oceanic concordance of phylogeography and biogeography: A case study in *Notochthamalus*. *Ecology and Evolution*, 6(13), 4403–4420.

- Foll, M., & Gaggiotti, O. E. (2008). A genome scan method to identify selected loci appropriate for both dominant and codominant markers: A Bayesian perspective. *Genetics*, *180*, 977–993.
- Fraser, C. I., Morrison, A. K., Hogg, A. M., Macaya, E. C., van Sebille, E., Ryan, P. G., Padovan, A., Jack, C., Valdivia, N., & Waters, J. M. (2018). Antarctica's ecological isolation will be broken by storm-driven dispersal and warming. *Nature Climate Change*, *8*, 704–708.
- Fraser, C. I., Nikula, R., & Waters, J. M. (2011). Oceanic rafting by a coastal community. *Proceedings of the Royal Society B*, *278*, 649–655.
- Fraser, C. I., Velásquez, M., Nelson, W. A., Macaya, E. C., & Hay, C. H. (2020). The biogeographic importance of buoyancy in macroalgae: A case study of the southern bull-kelp genus *Durvillaea* (Phaeophyceae), including descriptions of two new species. *Journal of Phycology*, *56*(1), 23–36.
- Frichot, E., & François, O. (2015). LEA: An R package for landscape and ecological association studies. *Methods in Ecology and Evolution*, *6*(8), 925–929.
- Gilbertson, C. R., & Wyatt, J. D. (2016). Evaluation of euthanasia techniques for an invertebrate species, land snails (*Succinea putris*). *Journal of the American Association for Laboratory Animal Science*, *55*(5), 577–581.
- Goldstien, S. J., Schiel, D. R., & Gemmill, N. J. (2006). Comparative phylogeography of coastal limpets across a marine disjunction in New Zealand. *Molecular Ecology*, *15*(11), 3259–3268.
- González, A., Beltrán, J., Hiriart-Bertrand, L., Flores, V., de Reviers, B., Correa, J. A., & Santelices, B. (2012). Identification of cryptic species in the lessonia nigrescens complex (phaeophyceae, laminariales). *Journal of Phycology*, *48*(5), 1153–1165.
- Goudet, J., & Jombart, T. (2021). *hierfstat: Estimation and tests of hierarchical F-statistics*. R package version 0.5-10. <https://CRAN.R-project.org/package=hierfstat>
- Gray, J. E. (1847). A list of the genera of recent Mollusca, their synonymy and types. *Proceedings of the Zoological Society of London*, *15*, 129–219.
- Guiñez, R., Pita, A., Pérez, M., Briones, C., Navarrete, S. A., Toro, J., & Presa, P. (2016). Present-day connectivity of historical stocks of the ecosystem engineer *Perumytilus purpuratus* along 4500 km of the Chilean coast. *Fisheries Research*, *179*, 322–332.
- Gutenkunst, R., Hernandez, R., Williamson, S., & Bustamante, C. (2010). Diffusion approximations for demographic inference: DaDi. *Nature Precedings*, *5*, 1.
- Haye, P. A., Segovia, N. I., Muñoz-Herrera, N. C., Gálvez, F. E., Martínez, A., Meynard, A., Pardo-Gandarillas, M. C., Poulin, E., & Faugeron, S. (2014). Phylogeographic structure in benthic marine invertebrates of the southeast pacific coast of Chile with differing dispersal potential. *PLoS One*, *9*(2), 1–15.
- Haye, P. A., Segovia, N. I., Varela, A. I., Rojas, R., Rivadeneira, M. M., & Thiel, M. (2019). Genetic and morphological divergence at a biogeographic break in the beach-dwelling brooder *Excirrolana hirsuticauda* Menzies (Crustacea, Peracarida). *BMC Evolutionary Biology*, *19*(1), 118.
- Hettinger, A., Sanford, E., Hill, T. M., Lenz, E. A., Russell, A. D., & Gaylord, B. (2013). Larval carry-over effects from ocean acidification persist in the natural environment. *Global Change Biology*, *19*, 3317–3326.
- Hijmans, R. J. (2021). *geosphere: Spherical trigonometry*. R package version 1.5-14. <https://CRAN.R-project.org/package=geosphere>
- Hoang, D. T., Vinh, L. S., Flouri, T., Stamatakis, A., von Haeseler, A., & Minh, B. Q. (2018). MPBoot: Fast phylogenetic maximum parsimony tree inference and bootstrap approximation. *BMC Evolutionary Biology*, *18*(1), 1–11.
- Hormazabal, S., Shaffer, G., & Leth, O. K. (2004). Coastal transition zone off Chile. *Journal of Geophysical Research*, *109*(C1), C01021.
- Jombart, T., & Ahmed, I. (2011). *Adegenet 1.3-1*: New tools for the analysis of genome-wide SNP data. *Bioinformatics*, *27*(21), 3070–3071.
- Jouganous, J., Long, W., Ragsdale, A. P., & Gravel, S. (2017). Inferring the joint demographic history of multiple populations: Beyond the diffusion approximation. *Genetics*, *206*(3), 1549–1567.
- Kaiser, J., Lamy, F., & Hebbeln, D. (2005). A 70-kyr sea surface temperature record off southern Chile (Ocean Drilling Program Site 1233). *Paleoceanography*, *20*(4), 1–15.
- Kalyaanamoorthy, S., Minh, B. Q., Wong, T. K., Von Haeseler, A., & Jermini, L. S. (2017). Model Finder: Fast model selection for accurate phylogenetic estimates. *Nature Methods*, *14*(6), 587–589.
- Kamvar, Z. N., Tabima, J. F., & Grünwald, N. J. (2014). Poppr: An R package for genetic analysis of populations with clonal, partially clonal, and/or sexual reproduction. *PeerJ*, *2*, e281.
- Kay, M. C., & Emlet, R. B. (2002). Laboratory spawning, larval development, and metamorphosis of the limpets *Lottia digitalis*. *Invertebrate Biology*, *121*(1), 11–24.
- Kolbin, K. G., & Kulikova, V. A. (2011). Reproduction and larval development of the limpet *Lottia persona* (Rathke, 1833) (Gastropoda: Lottiidae). *Russian Journal of Marine Biology*, *37*(3), 239–242.
- Kuo, E. S. L., & Sanford, E. (2013). Northern distribution of the seaweed limpet *Lottia insessa* (Mollusca: Gastropoda) along the Pacific coast. *Pacific Science*, *67*(2), 303–313.
- Langmead, B., & Salzberg, S. (2012). Fast gapped-read alignment with Bowtie 2. *Nature Methods*, *9*, 357–359.
- Lara, C., Saldías, G. S., Cazelles, B., Rivadeneira, M. M., Haye, P. A., & Broitman, B. R. (2019). Coastal biophysical processes and the biogeography of rocky intertidal species along the South-Eastern Pacific. *Journal of Biogeography*, *46*(2), 420–431.
- Lardies, M. A., Caballero, P., Duarte, C., & Poupin, M. J. (2021). Geographical variation in phenotypic plasticity of intertidal sister limpet's species under ocean acidification scenarios. *Frontiers in Marine Science*, *8*, 1–13.
- Largier, J. L. (2020). Upwelling bays: How coastal upwelling controls circulation, habitat, and productivity in bays. *Annual Review of Marine Science*, *12*, 415–447.
- Lesson, R. P. (1830). *Voyage autour du monde, sur la Corvette la Coquille, pendant les années 1822–1825. Voyage Coquille, Zoologie 2*.
- Letelier, J., Soto-Mardones, L., Salinas, S., Vincenti, L., Pavez, R., & Arriagada, M. (2012). Influencia de la península de mejillones en la variabilidad oceanográfica anual e interanual frente al norte de Chile. *Revista de Biología Marina y Oceanografía*, *47*(3), 513–526.
- López, B. A., Macaya, E. C., Jeldres, R., Valdivia, N., Bonta, C. C., Tala, F., & Thiel, M. (2018). Spatio-temporal variability of strandings of the southern bull kelp *Durvillaea Antarctica* (Fucales, Phaeophyceae) on beaches along the coast of Chile linked to local storms. *Journal of Applied Phycology*, *31*(3), 2159–2173.
- Manel, S., Guerin, P. E., Mouillot, D., Blanchet, S., Velez, L., Albouy, C., & Pellissier, L. (2020). Global determinants of freshwater and marine fish genetic diversity. *Nature Communications*, *11*, 692.
- McGaughran, A., Liggins, L., Marske, K. A., Dawson, M. N., Schiebelhut, L. M., Lavery, S., Knowles, L., Moritz, C., & Riginos, C. (2022). Comparative Phylogeography in the genomic age: Opportunities and challenges. *Journal of Biogeography*, *49*, 2130–2144.
- Navarrete, S. A., Broitman, B. R., & Menge, B. A. (2008). Interhemispheric comparison of recruitment to intertidal communities: Pattern persistence and scales of variation. *Ecology*, *89*(5), 1308–1322.
- Navarrete, S. A., Wieters, E. A., Broitman, B. R. R., & Castilla, J. C. (2005). Scales of benthic-pelagic coupling and the intensity of species interactions: From recruitment limitation to top-down control. *Proceedings of the National Academy of Sciences of the United States of America*, *102*(50), 18046–18051.
- Nguyen, L. T., Schmidt, H. A., Von Haeseler, A., & Minh, B. Q. (2015). IQ-TREE: A fast and effective stochastic algorithm for estimating maximum-likelihood phylogenies. *Molecular Biology and Evolution*, *32*(1), 268–274.
- Noskova, E., Ulyantsev, V., Koepfli, K. P., O'Brien, S. J., & Dobrynin, P. (2020). GADMA: Genetic algorithm for inferring demographic

- history of multiple populations from allele frequency spectrum data. *GigaScience*, 9(3), g1aa005.
- Oksanen, J., Blanchet, F. G., Friendly, M., Kindt, R., Legendre, P., McGlinn, D., Minchin, P. R., O'Hara, R. B., Simpson, G. L., Solymos, P., Stevens, M. H., Szoecs, E., & Wagner, H. (2020). *vegan: Community ecology package*. R package version 2.5-7. <https://CRAN.R-project.org/package=vegan>
- O'Leary, S. J., Puritz, J. B., Willis, S. C., Hollenbeck, C. M., & Portnoy, D. S. (2018). These aren't the loci you'e looking for: Principles of effective SNP filtering for molecular ecologists. *Molecular Ecology*, 27(16), 3193–3206.
- Orbigny, A. D. (1841). Voyage dans l'Amérique méridionale. *Mollusques*, 5, 409–488.
- Page, L. R. (2002). Apical sensory organ in larvae of the patellogastropod *Tectura scutum*. *Biological Bulletin*, 202(1), 6–22.
- Pantoja, S., Iriarte, J. L., & Daneri, G. (2011). Oceanography of the Chilean Patagonia. *Continental Shelf Research*, 31(3–4), 149–153.
- Paris, J. R., Stevens, J. R., & Catchen, J. M. (2017). Lost in parameter space: A road map for stacks. *Methods in Ecology and Evolution*, 8(10), 1360–1373.
- Privé, F., Luu, K., Vilhjálmsson, B. J., & Blum, M. G. (2020). Performing highly efficient genome scans for local adaptation with R package pcadapt version 4. *Molecular Biology and Evolution*, 37(7), 2153–2154.
- Quesada-Calderón, S., Giles, E. C., Morales-González, S., & Saenz-Agudelo, P. (2021). Pinpointing genetic breaks in the southeastern Pacific: Phylogeography and genetic structure of a commercially important tunicate. *Journal of Biogeography*, 48(10), 2604–2615.
- Ragionieri, L., Fratini, S., Vannini, M., & Schubart, C. D. (2009). Phylogenetic and morphometric differentiation reveal geographic radiation and pseudo-cryptic speciation in a mangrove crab from the Indo-West Pacific. *Molecular Phylogenetics and Evolution*, 52(3), 825–834.
- Ramajo, L., Valladares, M., Astudillo, O., Fernández, C., Rodríguez-Navarro, A. B., Watt-Arévalo, P., Núñez, M., Grenier, C., Román, R., Aguayo, P., Lardies, M. A., Broitman, B. R., Tapia, P., & Tapia, C. (2020). Upwelling intensity modulates the fitness and physiological performance of coastal species: Implications for the aquaculture of the scallop *Argopecten purpuratus* in the Humboldt current system. *Science of the Total Environment*, 745, 140949.
- Riginos, C., & Liggins, L. (2013). Seascape genetics: Populations, individuals, and genes marooned and adrift. *Geography Compass*, 7(3), 197–216.
- Río Cardoza, C. F. (1992). *Dinámica del asentamiento larvario de Scurria scurra (Lesson, 1830) (Gastropoda: Acmaeidae) en el intermareal rocoso de Mehuín (X Región)*. [Master Dissertation, Facultad de Ciencias, Universidad Austral de Chile].
- Rivadeneira, M. M., Fernández, M., & Navarrete, S. A. (2002). Latitudinal trends of species diversity in rocky intertidal herbivore assemblages: Spatial scale and the relationship between local and regional species richness. *Marine Ecology Progress Series*, 245, 123–131.
- Rodríguez-Romero, A., Gaitán-Espitia, J. D., Opitz, T., & Lardies, M. A. (2022). Heterogeneous environmental seascape across a biogeographic break influences the thermal physiology and tolerances to ocean acidification in an ecosystem engineer. *Diversity and Distributions*, 28, 1542–1553.
- Roughan, M., Mace, A. J., Largier, J. L., Morgan, S. G., Fisher, J. L., & Carter, M. L. (2005). Subsurface recirculation and larval retention in the lee of a small headland: A variation on the upwelling shadow theme. *Journal of Geophysical Research, C: Oceans*, 110(10), 1–18.
- Saenz-Agudelo, P., Peluso, L., Nespolo, R., Broitman, B. R., Haye, P. A., & Lardies, M. A. (2022). Population genomic analyses reveal hybridization and marked differences in genetic structure of *Scurria* limpet sister species with parapatric distributions across the south eastern Pacific. *Ecology and Evolution*, 12(5), 1–13.
- Saldías, G. S., Largier, J. L., Mendes, R., Pérez-Santos, I., Vargas, C. A., & Sobarzo, M. (2016). Satellite-measured interannual variability of turbid river plumes off Central-Southern Chile: Spatial patterns and the influence of climate variability. *Progress in Oceanography*, 146, 212–222.
- Saldías, G. S., Sobarzo, M., & Quiñones, R. (2019). Freshwater structure and its seasonal variability off western Patagonia. *Progress in Oceanography*, 174, 143–153.
- Sánchez, R., Sepúlveda, R. D., Brante, A., & Cárdenas, L. (2011). Spatial pattern of genetic and morphological diversity in the direct developer *Acanthina monodon* (Gastropoda: Mollusca). *Marine Ecology Progress Series*, 434, 121–131.
- Selkoe, K. A., D'Aloia, C. C., Crandall, E. D., Iacchei, M., Liggins, L., Puritz, J. B., Von Der Heyden, S., & Toonen, R. J. (2016). A decade of seascape genetics: Contributions to basic and applied marine connectivity. *Marine Ecology Progress Series*, 554, 1–19.
- Sowerby, G. B. (1839). Molluscous animals and their shells. In F. W. Beechey (Ed.), *The zoology of captain Beechey's voyage to the Pacific and Behring's straits* (pp. 103–155). H. G. Bohn.
- Strub, P. T., James, C., Montecino, V., Rutllant, J. A., & Blanco, J. L. (2019). Ocean circulation along the southern Chile transition region (38°–46°S): Mean, seasonal and interannual variability, with a focus on 2014–2016. *Progress in Oceanography*, 172, 159–198.
- Swearer, S. E., Treml, E. A., & Shima, J. S. (2019). A review of biophysical models of marine larval dispersal. *Oceanography and Marine Biology*, 57, 325–356.
- Thiel, M., Macaya, E. C., Acuña, E., Arntz, W., Bastias, H., Brokordt, K., Camus, P., Castilla, J., Castro, L., Cortés, M., Dumont, C., Escribano, R., Miriam, F., Gajardo, J. A., Gaymer, C. F., Gómez, I., Gonzalez, A., González, H., Haye, P., ... Vega, J. (2007). The Humboldt current system of northern and Central Chile oceanographic processes, ecological interactions and socioeconomic feedback. *Oceanography and Marine Biology*, 45, 195–344.
- Valdivia, N., Aguilera, M. A., Navarrete, S. A., & Broitman, B. R. (2015). Disentangling the effects of propagule supply and environmental filtering on the spatial structure of a rocky shore metacommunity. *Marine Ecology Progress Series*, 538, 67–79.
- Valdovinos, C. (1999). Biodiversidad de moluscos chilenos: base de datos taxonómica y distribucional. *Gayana*, 63(2), 111–164.
- Vargas, C. A., Cuevas, L. A., Broitman, B. R., San Martin, V. A., Lagos, N. A., Gaitán-Espitia, J. D., & Dupont, S. (2020). Upper environmental pCO<sub>2</sub> drives sensitivity to ocean acidification in marine invertebrates. *Nature Climate Change*, 12(2), 200–207.
- Zakas, C., Binford, J., Navarrete, S. A., & Wares, J. P. (2009). Restricted gene flow in Chilean barnacles reflects an oceanographic and biogeographic transition zone. *Marine Ecology Progress Series*, 394(2), 165–177.
- Zheng, X., Levine, D., Shen, J., Gogarten, S., Laurie, C., & Weir, B. (2012). A high-performance computing toolset for relatedness and principal component analysis of SNP data. *Bioinformatics*, 28(24), 3326–3328.

## SUPPORTING INFORMATION

Additional supporting information can be found online in the Supporting Information section at the end of this article.

**How to cite this article:** Peluso, L., Broitman, B. R., Lardies, M. A., Nespolo, R. F., & Saenz-Agudelo, P. (2023).

Comparative population genetics of congeneric limpets across a biogeographic transition zone reveals common patterns of genetic structure and demographic history. *Molecular Ecology*, 00, 1–14. <https://doi.org/10.1111/mec.16978>